ORIGINAL ARTICLE EXPERIMENTAL ALLERGY AND IMMUNOLOGY

Protective role of palmitoylethanolamide in contact allergic dermatitis

S. Petrosino[1,2,3], L. Cristino[1,4], M. Karsak[5], E. Gaffal[6], N. Ueda[7], T. Tüting[6], T. Bisogno[1,2], D. De Filippis[8], A. D'Amico[8], C. Saturnino[3], P. Orlando[1,9], A. Zimmer[5], T. Iuvone[1,8] & V. Di Marzo[1,2]

[1]Endocannabinoid Research Group; [2]Institute of Biomolecular Chemistry, C.N.R., Pozzuoli (Naples), Italy; [3]Department of Pharmaceutical Sciences, University of Salerno, Fisciano (Salerno), Italy; [4]Institute of Cybernetics, C.N.R., Pozzuoli (Naples), Italy; [5]Department of Molecular Psychiatry, University of Bonn, Germany; [6]Laboratory of Experimental Dermatology, University of Bonn, Bonn, Germany; [7]Department of Biochemistry School of Medicine, Kagawa University, Kagawa, Japan; [8]Department of Experimental Pharmacology, University of Naples "Federico II", Naples, Italy; [9]Institute of Protein Biochemistry, C.N.R., Naples, Italy

To cite this article: Petrosino S, Cristino L, Karsak M, Gaffal E, Ueda N, Tüting T, Bisogno T, De Filippis D, D'Amico A, Saturnino C, Orlando P, Zimmer A, Iuvone T, Di Marzo V. Protective role of palmitoylethanolamide in contact allergic dermatitis. *Allergy* 2010; **65**: 698–711.

Keywords
chemokines; contact allergens; dermatology; dermatology contact dermatitis; pharmacology.

Correspondence
Vincenzo Di Marzo, Via Campi Flegrei 34, Comprensorio Olivetti, 80078 Pozzuoli (Naples), Italy.

Accepted for publication 30 September 2009

DOI:10.1111/j.1398-9995.2009.02254.x

Editor: Thomas Bieber

Abstract

Background: Palmitoylethanolamide (PEA) is an anti-inflammatory mediator that enhances the activation by anandamide (AEA) of cannabinoid receptors and transient receptor potential vanilloid type-1 (TRPV1) channels, and directly activates peroxisome proliferator-activated receptor-α (PPAR-α). In mice, 2,4-dinitrofluorobenzene (DNFB)-induced contact allergic dermatitis (CAD) in inflamed ears is partly mediated by the chemokine Monocyte Chemotactic Protein-2 (MCP-2) and accompanied by elevation of AEA levels. No datum is available on PEA regulation and role in CAD.
Objective: We examined whether PEA is produced during DNFB-induced CAD, and if it has any direct protective action in keratinocytes *in vitro*.
Methods: Eight- to ten-week-old female C57BL/6J wild-type and CB_1/CB_2 double knock-out mice were used to measure PEA levels and the expression of TRPV1, PPAR-α receptors and enzymes responsible for PEA biosynthesis and degradation. Human keratinocytes (HaCaT) cells were stimulated with polyinosinic polycytidylic acid [poly-(I:C)], and the expression and release of MCP-2 were measured in the presence of PEA and antagonists of its proposed receptors.
Results: 2,4-Dinitrofluorobenzene increased ear skin PEA levels and up-regulated TRPV1, PPAR-α and a PEA-biosynthesizing enzyme in ear keratinocytes. In HaCaT cells, stimulation with poly-(I:C) elevated the levels of both PEA and AEA, and exogenous PEA (10 μM) inhibited poly-(I:C)-induced expression and release of MCP-2 in a way reversed by antagonism at TRPV1, but not PPAR-α. PEA (5–10 mg/kg, intraperitoneal) also inhibited DNFB-induced ear inflammation in mice *in vivo*, in a way attenuated by TRPV1 antagonism.
Conclusions: We suggest that PEA is an endogenous protective agent against DNFB-induced keratinocyte inflammation and could be considered for therapeutic use against CAD.

Contact allergic dermatitis (CAD) is an inflammatory condition of the skin defined as a delayed hypersensitivity reaction that occurs after repeated exposure to an allergen. CAD can be induced by numerous irritants and/or allergens (nickel, rubber, plants, medications) and the corresponding rash develops within 48–72 h of re-exposure to the same antigen. Additional symptoms are itching, redness, swelling and the formation of small skin blisters. CAD develops in two steps: (1) contact of an allergen with the skin and its binding to Langerhans cells, which then travel to lymph nodes, where the allergen is exposed to T-lymphocytes; the allergen is also taken up by resident and newly recruited dendritic cells,

Abbreviations
CAD, contact allergic dermatitis; DNFB, 2,4-dinitrofluorobenzene; PEA, palmitoylethanolamide; poly-(I:C), polyinosinic acid-polycytidylic acid; TRPV1, transient receptor potential vanilloid type-1.

which migrate to lymph nodes and prime the T-lymphocytes; and (2) re-exposure to the allergen, which causes the activation of primed T-lymphocytes, with subsequent release of inflammatory mediators that are responsible for the features of inflammation and keratinocyte injury (1, 2).

Palmitoylethanolamide (PEA) is an endogenous lipid produced by most mammalian cells (3–5) and exhibiting anti-inflammatory and anti-nociceptive properties (6–10). It is biosynthesized from a phospholipid precursor, *N*-palmitoyl-phosphatidylethanolamine, through the catalytic action of *N*-acyl-phosphatidylethanolamine-selective phospholipase D (NAPE-PLD) (11). PEA inactivation to palmitic acid and ethanolamine can be catalysed by fatty acid amide hydrolase (FAAH) (12, 13) and, more specifically, by *N*-acylethanolamine-hydrolysing acid amidase (NAAA) (14, 15). The molecular mechanism of action of PEA is still controversial and several hypotheses have been put forward to explain its anti-inflammatory and analgesic effects. These hypotheses include the following: (1) an autacoid local inflammation antagonism mechanism through which PEA acts by down-regulating mast-cell degranulation (16–19); (2) the direct stimulation of the cannabinoid CB_2 receptor or of an as-yet uncharacterized CB_2-like receptor, as suggested by results obtained in different *in vivo* studies using the CB_2 antagonist SR144528 (6, 8, 20, 21) (but see below); (3) an 'entourage effect' (22, 23), through which PEA acts by enhancing the anti-inflammatory and anti-nociceptive effects exerted by another fatty acid ethanolamide, anandamide (AEA), which is often produced together with PEA. AEA acts by activating the cannabinoid CB_1 and CB_2 or the transient receptor potential vanilloid receptor type 1 (TRPV1) channel, and PEA might potentiate these actions either via inhibition of the expression of FAAH (24), for which AEA is also a substrate, or through allosteric stimulation of TRPV1 receptors (25–27), or both (28). Activation of TRPV1 receptors is then immediately followed by their desensitization and refractoriness to subsequent stimulation by inflammatory or nociceptive stimuli (29–31); (4) last, a specific molecular target has been found for PEA, the nuclear peroxisome proliferator-activated receptor-α (PPAR-α), which clearly mediates several anti-inflammatory effects of this compound (32). Interestingly, it was found that the CB_2 antagonist SR144528, previously described to antagonize PEA analgesic and anti-inflammatory effects (see above), also antagonizes PPAR-α (33), thus arguing against a role of CB_2 receptors in these actions.

A number of studies have shown the involvement of the cannabinoid and TRPV1 receptors in animal models of CAD (34). The levels of the other most studied endocannabinoid, 2-arachidonoylglycerol (2-AG), are markedly elevated in the ears following a challenge with oxazolone in sensitized mice (35). The swelling following the challenge is suppressed by the administration of SR144528, a CB_2 receptor antagonist, either immediately after sensitization, or upon the challenge. Moreover, the treatment with SR144528 suppresses the expression of mRNAs for pro-inflammatory cytokine, Monocyte Chemotactic Protein-1 and tumour necrosis factor-α, following a challenge with oxazolone. These results suggest that activation of CB_2 receptors by 2-AG might contribute to oxazolone-induced CAD (35), and are in agreement with previous data showing that SR144528 and another inverse agonist, JTE-907, reduce carrageenan-induced mouse paw oedema (36) and cutaneous inflammation induced by 2,4-dinitrofluorobenzene (DNFB) (37). By contrast, Karsak et al. (38) demonstrated that DNFB-treated mice lacking both CB_1 and CB_2 receptors exhibit exacerbated allergic ear inflammation, and that AEA and 2-AG levels are elevated in the ears of both wild-type (WT) mice and, particularly, CB_1/CB_2 double knock-out DNFB-treated mice. CB_1 and CB_2 receptors antagonists, SR141716A (Rimonabant) and SR144528, respectively, also exacerbate allergic inflammation, whereas the CB_1/CB_2 receptor agonist, Δ^9-tetra-hydrocannabinol attenuates inflammation by down-regulating the expression in keratinocytes of the chemokine MCP-2 (38). These results established a protective role of the endocannabinoid system during CAD. Finally, there is also evidence for a protective role of the vanilloid TRPV1 receptor in oxazolone-induced CAD in mice (39).

The aim of the present study was to investigate whether, similar to AEA and 2-AG (38), also PEA is produced during CAD to exert a protective action on keratinocytes via MCP-2 down-regulation. Therefore, we have first measured PEA concentrations in the ears of DNFB-treated WT and CB_1/CB_2 double knockout (KO) mice, and the expression, in keratinocytes, of its two proposed direct or indirect targets, PPAR-α and TRPV1, and biosynthetic and degrading enzymes, NAPE-PLD and NAAA, respectively. Next, we have investigated the formation and possible MCP-2-down-regulatory effects of PEA in cultured human keratinocytes (HaCaT) challenged with polyinosinic acid-polycytidylic acid [poly-(I:C)]. Finally, we have studied *in vivo* in WT mice the effect of PEA systemic administration on DNFB-induced ear inflammation and MCP-2 expression.

Materials and methods

Chemicals

2,4-Dinitrofluorobenzene was purchased from Sigma-Aldrich (Milano, Italy). Capsazepine (cpz), iodio-resiniferatoxin (I-RTX) and MK-886 were purchased from Tocris (Bristol, UK). poly-(I:C) was purchased from Invivogen (Labogen S.r.l., Milano, Italy). PEA and SR144528 were a gift from Epitech group S.r.l. (Padova, Italy) and Sanofi-Aventis (Montpellier, France), respectively. Cell culture media and antibiotics were purchased from Sigma-Aldrich. Human MCP-2 ELISA kit was purchased from RayBiotech, Inc (Tebu-Bio S.r.l., Milano, Italy).

Immunochemical normal sera, avidin–biotin kit, antigen unmasking solution, mouse on mouse kit and biotinylated secondary antibodies were purchased from Vector Laboratories (Burlingame, CA, USA). The 3-3′diaminobenzidine (DAB) kit was purchased from Sigma-Aldrich. The rabbit anti-goat fluorochrome conjugated secondary antibody Alexa 546 was purchased from Invitrogen Molecular Probes (Paisley, UK). The anti-cytokeratin, anti-TRPV1, anti-PPARα

primary antibodies, and their respective immunizing peptides, were purchased from Santa Cruz Biotechnology (Santa Cruz, CA, USA). The anti-CB_2 primary antibody and related immunizing peptide were purchased from Abcam (Cambridge, UK) whereas anti-NAPE-PLD, anti-NAAA and the respective immunizing peptides were developed in the laboratory of Prof. Ueda (11, 40).

Animals

Eight- to ten-week-old female C57BL/6J mice were obtained from Harlan. CB_1/CB_2 double knock-out mice ($CB_1^{-/-}/CB_2^{-/-}$) and their WT controls (CTRL) were bred at our animal facility in Bonn. Animal experiments were approved by the Bezirksregierung Köln, Germany and by the University of Naples, Federico II. The institutional and national guidelines for the care and use of laboratory animals were followed.

DNFB-induced CAD in mice

2,4-Dinitrofluorobenzene was diluted in acetone/olive oil (4 : 1) immediately before use. Mice were sensitized by painting 50 μl of 0.2% DNFB on the shaved abdomen on two consecutive days. Controls were treated with 50 μl acetone/olive oil. Ears of mice were painted with 10 μl of 0.3% DNFB on day 5. Ear thickness was measured 24, 48 and 72 h after challenge using an engineers micrometer, and ear swelling was calculated in each mouse as the difference in ear thickness between the unchallenged and the challenged ear. Statistical significances were evaluated with the Wilcoxon–Mann–Whitney two-samples test. After the second challenge and kill, the ears were removed and immediately immersed into liquid nitrogen, to be stored at −80° until extraction and purification of PEA. $N = 9$ mice per group were used for these experiments. These mice were the same that had been used previously for AEA and 2-AG level determination (38).

PEA measurement in the ears of DNFB-sensitized and challenged mice

Ears were homogenized in chloroform/methanol/Tris–HCl 50 mM pH 7.4 (2 : 1 : 1, v/v) containing 50 pmol of $[^2H]_4$-PEA as internal standard (41). The lipid-containing organic phase was dried down, weighed and prepurified by open-bed chromatography on silica gel. Fractions obtained by eluting the column with 9 : 1 (by vol) chloroform/methanol were analysed by liquid chromatography–atmospheric pressure chemical ionization–mass spectrometry (LC–APCI–MS) by using a Shimadzu HPLC apparatus (LC-10ADVP) coupled to a Shimadzu (LCMS-2010) quadrupole MS via a Shimadzu APCI interface (42). LC–APCI–MS analyses were carried out in the selected ion monitoring mode (43), using m/z values of 304 and 300 (molecular ions +1 for deuterated and undeuterated PEA). PEA levels were calculated on the basis of its area ratio with the internal deuterated standard signal area, its amount in pmols normalized per mg of lipids and compared by ANOVA followed by the Bonferroni's test. $N = 9$ mice per group were used for these experiments.

Immunohistochemical analysis for CB_2, TRPV1, PPAR-α, NAPE/PLD and NAAA

Paraffin-embedded ear skin of CTRL and DNFB-treated CB_1/CB_2 KO mice (KO/CTRL; KO/DNFB) and of the corresponding WT mice (WT/CTRL; WT/DNFB) were sectioned in five serial sections 6 μm thick and collected onto gelatine-coated slides. The ears used for these experiments were the same as those used previously to identify CB_2 receptors in keratinocytes (38). After de-paraffination, the first series was processed four double CB_2/cytokeratin immunoreactivity (ir); the second for TRPV1-ir, the third for PPAR-α-ir, the fourth for NAPE-PLD-ir and the fifth for NAAA-ir. All of the sections were processed with an antigen unmasking solution before the immunohistochemistry treatment, and then reacted in H_2O_2 (0.3%). Only the sections used for double CB_2/cytokeratin-ir were further processed with mouse immunodetection solution in order to prevent the nonspecific link between the mouse tissue and the monoclonal cytokeratin antibody. For the double CB_2/cytokeratin-ir, the sections were incubated in a normal donkey serum (NDS) mixture containing CB_2 rabbit polyclonal (1 : 50 in NDS) and cytokeratin monoclonal (1 : 300 in NDS) antibodies. The cytokeratin-ir was revealed through donkey anti-mouse IgGs (1 : 150 in NDS) and 0.05% DAB whereas the CB_2-ir was revealed through Alexa 546 donkey anti-rabbit IgGs (1 : 100 in NDS). All the sections were investigated under bright-field illumination for single cytokeratin-ir DAB immunostaining and in epifluorescence light for CB_2-ir immunofluorescence (Leica Microsystems Wetzlar GmbH, Wetzlar, Germany). For TRPV1-ir or PPAR-α-ir, the sections were incubated for 1 h in normal rabbit serum (NRS) and overnight at +4°C with primary goat polyclonal TRPV1 or PPAR-α antibodies (1 : 200 in NRS). Subsequently, the sections were incubated for 2 h in biotinylated rabbit anti-goat IgGs [1 : 100 in normal goat serum (NGS)]. For NAPE-PLD-ir or NAAA-ir, the sections were incubated for 1 h in NGS and overnight at +4°C with primary rabbit polyclonal NAPE-PLD or NAAA antibodies (1 : 250 in NGS). Subsequently, the sections were incubated for 2 h in biotinylated goat anti-rabbit IgGs (1 : 100 in NGS), processed with avidin–biotin–peroxidase solution and then in 0.05% DAB. Finally, all sections were washed in water, dehydrated, cleared in xylene, mounted in DPX and observed under bright-field illumination (Leica DM IRB microscope). Images were acquired using the image analysis software LEICA IM500 and the digital camera Leica DFC 320 connected to the microscope. The sections processed for immunofluorescence were studied with an epifluorescence microscope (Leica DM IRB); settings for excitation of fluorochrome 546 nm was identical throughout the analysis. Images were processed in Adobe Photoshop, with brightness and contrast being the only adjustments made. Immunohistochemical CTRL included pre-absorption of diluted antibodies with the respective immunizing peptides or omission of either the primary antisera or the secondary antibodies. These CTRL experiments did not show any staining. $N = 3$ mice per group were used for these experiments.

Cell culture and treatments

The immortalized HaCaT cells were cultured in Dulbecco's Modified Eagle Medium (DMEM) supplemented with glutamine (2 mM), penicillin (400 U/ml), streptomycin (50 mg/ml) and 10% foetal bovine serum in a humidified 5% CO_2 atmosphere at 37°C. For sensitization, cells were plated into six-well culture plates at a cell density of 7×10^4 cells per well, and after 1 day were stimulated with poly-(I:C) (100 μg/ml) or vehicle (water) and incubated for 24 h at 37°C in 5% CO_2. To study the effect of PEA or vehicle, poly-(I:C)-treated HaCaT cells were treated with PEA (0.1–1–10 μM) or solvent (methanol, max 0.1%) and incubated for the indicated times. To study the effect of antagonists, poly-(I:C)-treated HaCaT cells were treated with SR144528 (0.5 μM), I-RTX (0.1 μM), MK-886 (10 μM) in presence or in absence of PEA (10 μM) for the indicated time periods. SR144528 and MK-886 were dissolved in methanol, and I-RTX in dimethyl sulfoxide.

Cells plated on slide (Deckglaser, 21 × 26 mm) into six-well culture plates after 24 h were used for MCP-2 chemokine immunocytochemical analysis. Cells plated into six-well culture plates after 6 h were used for MCP-2 RT-PCR analysis, whereas supernatants were used for MCP-2 ELISA assay.

Immunocytochemical analysis of MCP-2

Human keratinocytes cells plated on slide (Deckglaser, 21 × 26 mm) into six-well culture plates after 24 h were used for MCP-2 immunocytochemical reactions in vehicle (VEH) *vs* poly-(I:C)-treated cells, VEH *vs* PEA-treated cells (0.1–1–10 μM), poly-(I:C) and PEA co-stimulated cells (0.1–1–10 μM), poly-(I:C) or PEA or poly-(I:C) + PEA *vs* SR144528- (0.5 μM) or I-RTX- (0.1 μM) or MK-886- (10 μM) treated cells. After removal of cell culture media and three brief and delicate rinses in phosphate buffer solution (pH = 7.4, 0.1 M), the cells attached on slides were fixed in paraformaldehyde solution (4% in PB on agitation at +4°C) then washed in PB and incubated in for 1 h in NGS and overnight with primary rabbit polyclonal MCP-2 antibody (1 : 300 in NGS). Subsequently, the cells were incubated for 2 h in biotinylated goat anti-rabbit IgGs (1 : 150 in NGS), processed with avidin–biotin–peroxidase solution and then in 0.05% DAB, washed in water, dehydrated, cleared in xylene, mounted in DPX and observed under bright-field illumination. Images were acquired using the image analysis software LEICA IM500 and the digital camera Leica DFC 320 connected to the microscope. Images were processed in Adobe Photoshop, with brightness and contrast being the only adjustments made. Immunocytochemical CTRL included pre-absorption of diluted MCP-2 antibody with immunizing peptide or omission of either the primary antisera or the secondary antibody. These CTRL experiments did not show any staining.

Densitometric analysis of TRPV1, PPAR-α, NAPE-PLD, NAAA and MCP-2 immunostaining

Quantitative analysis of intensity of immunostaining was performed for TRPV1, PPAR-α, NAPE-PLD and NAAA in the ear skin and for MCP-2 in HaCaT keratinocytes by using a digital camera working on grey levels (JCV FC 340FX; Leica) and a software IMAGE PRO PLUS® 6.0 for Windows, MediaCybernetics Inc. (Bethesda, MD, USA), working on logarithmic values scale of absorbance for densitometric evaluation. All densitometric measures were performed on the tissue or cells processed for immunoperoxidase reaction by an observer blind to the experimental treatment being analysed. For densitometric analyses, a sample of 100 ± 5 immunopositive cells with nuclei (unstained or lightly stained) in the focal plane were randomly identified for each animal from $n = 3$ animals per group, in the case of histological samples, or for each immunological trail from $n = 3$ trials, in the case of cytochemical samples. The images were acquired under constant light illumination and at the same magnification. In each section, the zero value of optical density was assigned to the background, i.e. a portion of sample devoid of stained cell bodies. The average values were compared by means of analysis of variance (one-way ANOVA) followed by the Bonferroni's test.

RT-PCR analyses

Total RNA was extracted from either tissue or cells in RNA later, analysed by a 2100 Bioanalyzer (Agilent Technologies, Waldbronn, Germany) (RNA integrity number > 7.0) and retro-transcribed as previously described (44). RNA from CTRL and inflamed ears was obtained from small specimens (5 mg wet tissue weight) of ear skin coming from the experiments carried out both during a previous study (38) and in the present study. Quantitative PCR analysis was performed essentially as described by an iCycler-iQ5® (Bio-Rad Laboratories, Hercules, CA, USA) in a 25 μl reaction mixture containing 10–50 ng of cDNA Optimized primers for SYBR®-Green analysis (accession numbers: MCP-2, NM_005623; CB2, NM_009924; TRPV1, NM_001001445; PPAR-α, NM_011144.6; NAPE-PLD, AB112350; NAAA, NM_025972.4; FAAH, NM_010173) and optimum annealing temperatures were designed by ALLELE-LD® software version 6.0 (Biosoft International, Palo Alto, CA, USA) and were synthesized (HPLC-purification grade) by Eurofins/MWG GMBH (Ebersberg, Germany). Assays were performed in quadruplicate (Δ from threshold cycle of replicate samples < 0.3) and a standard curve from consecutive fivefold dilutions (100–0.16 ng) of a cDNA pool representative of all samples was included, for PCR-efficiency determination. Relative gene expression analysis, corrected for PCR-efficiency and normalized respect to reference gene β-actin (accession: NM_001101), was performed by the ICYCLER-IQ5 software (Bio-Rad Laboratories, Hercules, CA, USA) 'Gene expression module'. Significance was evaluated according to Pfaffl et al. (45).

ELISA assay

MCP-2 levels were measured from cell supernatants derived from poly-(I:C)-treated HaCaT cells, with or without the TRPV1 antagonist, I-RTX, in presence or in absence of PEA

using the human MCP-2 ELISA kit protocol and according to the manufacture's instructions (Ray Biotech, Inc. provided by Tebu-Bio, Magenta, Milan, Italy).

Endocannabinoid, PEA and oleoylethanolamide (OEA) measurement in poly-(I:C)-sensitized HaCaT cells

Human keratinocytes cells were plated into six-well culture plates and sensitized with poly-(I:C). After 24 h, cells and supernatants were homogenized in chloroform/methanol/Tris–HCl 50 mM pH 7.4 (2 : 1 : 1, v/v) containing 10 pmol of $[^2H]_8$-AEA, and 50 pmol of $[^2H]_5$-2AG, $[^2H]_4$-PEA and $[^2H]_2$-OEA as internal standards (41). The extraction and purification phases and the LC–APCI–MS analysis of PEA were conducted as described earlier. LC–APCI–MS analysis of AEA, 2-AG and OEA analysis were carried out using m/z values of 356 and 348 (molecular ions +1 for deuterated and undeuterated AEA), 384.35 and 379.35 (molecular ions +1 for deuterated and undeuterated 2-AG), 328 and 326 (molecular ions +1 for deuterated and undeuterated OEA). AEA, 2-AG and OEA levels were calculated by isotopic dilution, as described for earlier for PEA.

Drugs and their administration to mice with DNFB-induced CAD

Palmitoylethanolamide (5 and 10 mg/kg), cpz (0.5 and 2 mg/kg) and the association of PEA, 5 mg/kg, and cpz, 0.5 mg/kg, or the association of PEA, 10 mg/kg, and cpz, 2 mg/kg, were administered intraperitoneally (i.p.) on day 5, 6, 7 (the days of the first challenge with DNFB), or on day 12, 13, 14 (the days of the second challenge with DNFB) after the initial sensitization with DNFB. $N = 11$ mice per group were used for these experiments.

Results

PEA concentrations and MCP-2 mRNA levels in the ears of DNFB-sensitized/challenged mice

For these experiments, we employed exactly the same mouse ear extracts previously shown to contain elevated AEA and 2-AG levels following DNFB treatment and subsequent second challenge, and in which measures of ear thickness (oedema) had been already carried out (38). PEA amounts were measured by LC-MS in the ear skin of DNFB-sensitized mice after the second challenge with DNFB and induction of ear swelling. DNFB challenge caused in both WT and, particularly, double CB_1/CB_2 KO mice a significant increase in both ear thickness and ear MCP-2 mRNA levels assessed by q-PCR (see ref. 38 and Table 1). PEA levels were 29.9 ± 1.5 *vs* 36.5 ± 5.4 pmol/mg of lipid extract in vehicle-treated WT mice (WT/CTRL) *vs* DNFB-treated WT mice (WT/DNFB), and 33.5 ± 4.2 *vs* 97.8 ± 4.9 pmol/mg lipid extract in vehicle-treated $CB_1^{-/-}/CB_2^{-/-}$ KO mice (CB_1/CB_2 KO/CTRL) *vs* DNFB-treated $CB_1^{-/-}/CB_2^{-/-}$ mice (CB_1/CB_2 KO/DNFB) (Fig. 1). Thus, the higher the degree of inflammation (WT/CTRL ≤ CB_1/CB_2 KO/CTRL < WT/DNFB << CB_1/CB_2 KO/DNFB) in terms of ear thickness (38) and expression of MCP-2 mRNA (Table 1), the higher was the concentration of PEA in ear skin.

Table 1 MCP-2 transcriptional expression in ear skin of DNFB-sensitized and challenged mice. In the first series of experiments, MCP-2 mRNA was measured after the second challenge in both wild-type (WT) and double CB_1/CB_2 null (KO) mice. In the second series, MCP-2 mRNA was measured after the second challenge only in WT mice with or without concomitant intra-peritoneal (i.p.) administration of PEA (5 mg/kg, i.p.) (see Materials and methods). Total RNA was extracted and assayed by quantitative RT-PCR for MCP-2 and β-actin (reference gene), as described in Materials and methods

Condition	Mean threshold cycles	SD	Normalized relative expression	SD
WT	29.72	0.24	0.018	0.003
WT + DNFB	23.26	0.16	0.89*	0.12
CB_1/CB_2 KO	29.30	0.39	0.023	0.007
CB_1/CB_2 KO + DNFB	23.40	0.16	1.00*	0.13
WT	26.57	0.19	0.014	0.003
WT + DNFB	19.21	0.07	1.00*	0.08
WT DNFB + PEA	19.98	0.05	0.60**	0.02

Normalized relative expression, expression normalized to β-actin and relative to the expression in the sample with highest expression (1.00); SD, standard deviation; DNFB, 2,4-dinitrofluorobenzene; KO, knockout; PEA, palmitoylethanolamide.
*$P < 0.005$ *vs* corresponding WT; **$P < 0.05$ *vs* WT + DNFB.

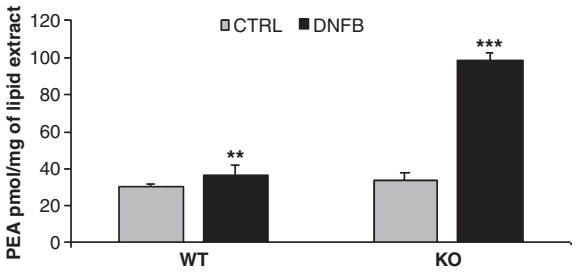

Figure 1 Endogenous palmitoylethanolamide levels in the ear skin of 2,4-dinitrofluorobenzene (DNFB)-sensitized and challenged mice, both in wild-type (WT) and in double CB_1/CB_2 knockout (KO) mice. Data are means ± SE of $N = 6$ separate determinations. **$P < 0.05$ for WT/control (CTRL) *vs* WT/DNFB; ***$P < 0.001$ for KO/CTRL *vs* KO/DNFB.

Potential targets of PEA are up-regulated in ear keratinocytes of DNFB-sensitized/challenged mice

To investigate whether the proposed receptors for PEA are localized in keratinocytes of the ears of DNFB-sensitized and challenged mice, we used the double immunohistochemical staining of CB_2 and cytokeratin on the de-paraffinated sections of the ears of DNFB-treated mice after the second challenge, coming from a previous study (38). DAB labelling

(cytokeratin-ir) and red fluorescence (CB_2-ir) revealed that the same dermal and epidermal cells are cytokeratin- and CB_2- ir (Fig. 2A). Likewise, TRPV1-ir as well as PPARα-ir (Fig. 2B,C) are over-expressed in what clearly look like keratinocytes of the ears of both WT mice and particularly, double CB_1/CB_2 KO mice after DNFB treatment, where the optical density of ir were: 0.41 ± 0.057 *vs* 0.50 ± 0.064 in WT/CTRL *vs* WT/DNFB, and 0.52 ± 0.049 *vs* 0.64 ± 0.077 in CB_1/CB_2 KO/CTRL *vs* CB_1/CB_2 KO/DNFB for TRPV1 receptors; and 0.36 ± 0.062 *vs* 0.49 ± 0.055 in WT/CTRL *vs* WT/DNFB, and 0.34 ± 0.079 *vs* 0.56 ± 0.059 in CB_1/CB_2 KO/CTRL *vs* CB_1/CB_2 KO/DNFB for PPAR-α receptors.

Expression of PEA metabolic enzymes in the ear keratinocytes of DNFB-sensitized/challenged mice

To investigate the possible cellular source of PEA in the ear skin of DNFB-treated mice and to assess whether its increased levels are accounted for by variations in the amounts of its biosynthetic and inactivating enzymes, we determined the levels of NAPE-PLD and NAAA (Fig. 3A,B), respectively, in the ear skin of DNFB-sensitized and challenged mice after the second challenge, coming from a previous study (38). NAPE-PLD protein expression was up-regulated, whereas NAAA protein expression was slightly

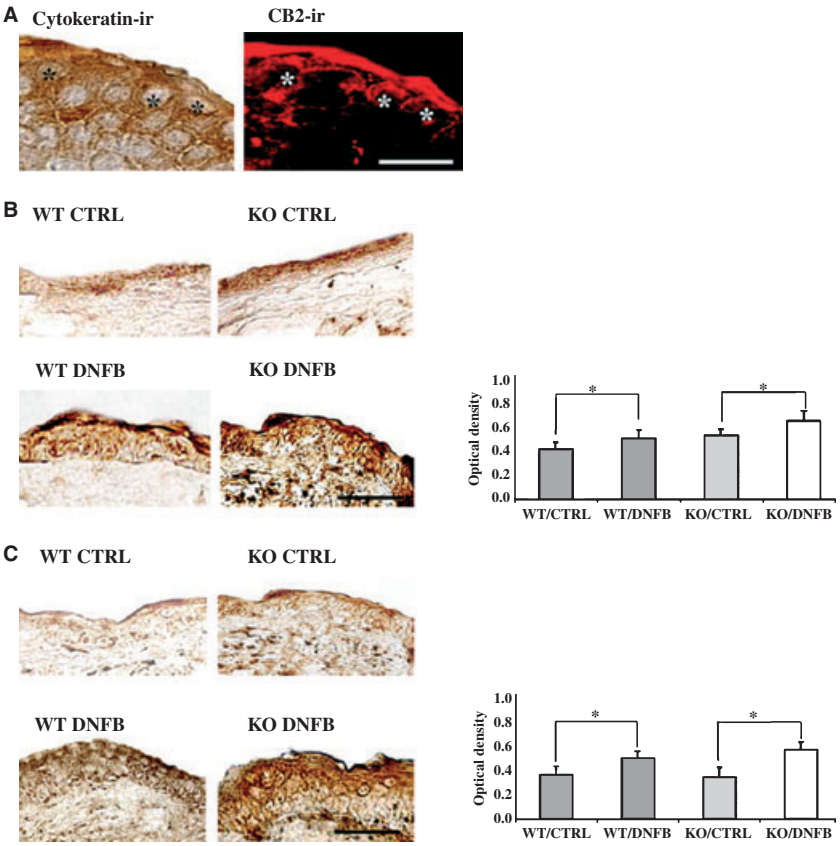

Figure 2 Expression of potential targets for palmitoylethanolamide in ear keratinocytes of mice treated with vehicle or sensitized and challenged with 2,4-dinitrofluorobenzene (DNFB). (A) 3-3′diaminobenzidine (DAB) labelling for cytokeratin-immunoreactivity (ir) and red fluorescence for CB_2-ir in keratinocytes of the ear skin in wild-type (WT) and DNFB-sensitized and challenged mice. The asterisks indicate the same cells double labelled with cytokeratin- and CB_2-ir. Scale bar = 60 μm. (B) Immunohistochemical analysis of transient receptor potential vanilloid type-1 (TRPV1) receptors expression in the ear skin of WT and knockout (KO) mice after DNFB treatment. In the DAB labelling for TRPV1-ir, note how TRPV1-ir increases in the keratinocytes of both WT mice and, particularly, in double CB_1/CB_2 KO mice after DNFB treatment (scale bar = 150 μm). This is confirmed by the corresponding densitometric analyses of TRPV1-ir, in which optical density is expressed in the log scale, and the data are means ± SD of $N = 3$ separate determinations on $n = 100$ cells. $^*P < 0.05$ for both WT/control (CTRL) *vs* WT/DNFB and for KO/CTRL *vs* KO/DNFB. (C) Immunohistochemical analysis of peroxisome proliferator-activated receptor-α (PPAR-α) receptors expression in the ear skin of WT and KO mice after DNFB treatment. In the DAB labelling for PPARα-ir, note how PPAR-α-ir increases in the keratinocytes of both WT mice and particularly, double CB_1/CB_2 KO mice after DNFB treatment (scale bar = 150 μm). This is confirmed by the corresponding densitometric analyses of PPAR-α-ir, in which optical density is expressed in the log scale, and the data are means ± SD of $N = 3$ separate determinations on $n = 100$ cells. $^*P < 0.05$ for both WT/CTRL *vs* WT/DNFB and KO/CTRL *vs* KO/DNFB.

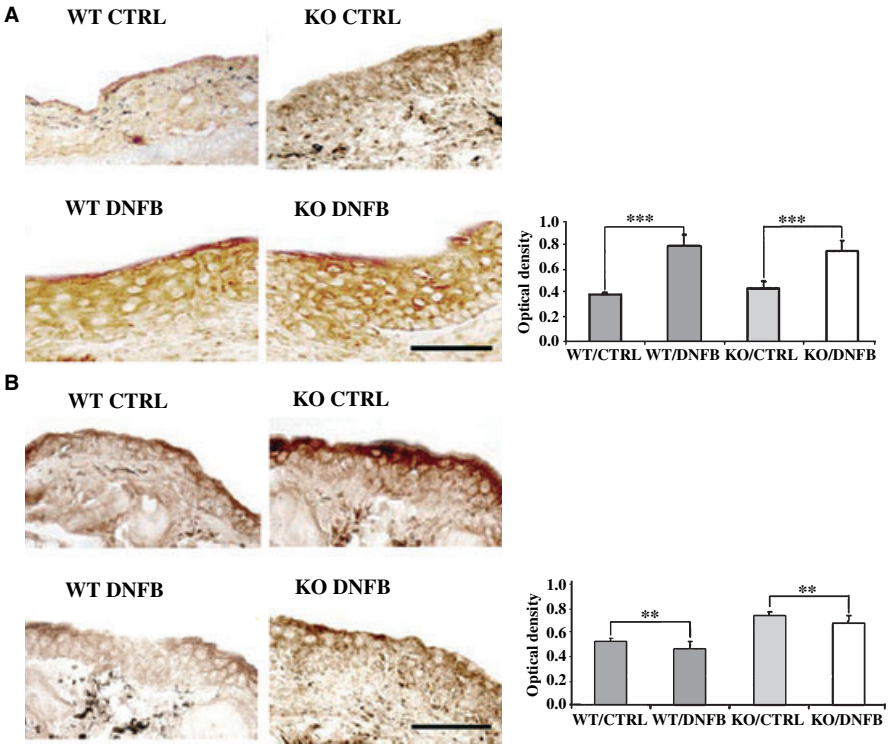

Figure 3 Expression of potential palmitoylethanolamide biosynthetic and degrading enzymes in ear keratinocytes of mice treated with vehicle or sensitized and challenged with 2,4-dinitrofluorobenzene (DNFB). (A) Immunohistochemical analysis of *N*-acyl-phosphatidylethanolamine-selective phospholipase D (NAPE-PLD) enzyme expression in the ear skin of wild-type (WT) and knockout (KO) mice after DNFB treatment. In the 3-3′diaminobenzidine (DAB) labelling for NAPE-PLD-immunoreactivity (ir), note the intense NAPE-PLD expression in keratinocytes of WT mice as well as in CB_1/CB_2 double KO mice, following DNFB treatment (scale bar = 150 μm). In the corresponding histograms of densitometric analyses of NAPE-PLD-ir, the optical density is expressed in the log scale, and the data are means ± SD of $N = 3$ separate determinations on $n = 100$ cells. $^{***}P < 0.001$ for both WT/control (CTRL) *vs* WT/DNFB and KO/CTRL *vs* KO/DNFB. (B) Immunohistochemical analysis of *N*-acylethanolamine-hydrolysing acid amidase (NAAA) enzyme expression in the ear skin of WT and KO mice after DNFB treatment. In the DAB labelling for NAAA-ir, note the lower NAAA-ir expression in keratinocytes of WT mice as well as in CB_1/CB_2 double KO mice, following DNFB treatment (scale bar = 150 μm). In the corresponding histograms of densitometric analyses of NAAA-ir, note that the optical density is expressed in the log scale, and the data are means ± SD of $N = 3$ separate determinations on $n = 100$ cells. $^{**}P < 0.005$ for both WT/CTRL *vs* WT/DNFB and KO/CTRL *vs* KO/DNFB.

down-regulated, in what clearly look like keratinocytes (Fig. 3A,B) of WT mice and CB_1/CB_2 double KO mice, following DNFB treatment, as shown by optical density of ir: 0.41 ± 0.011 *vs* 0.81 ± 0.097 in WT/CTRL *vs* WT/DNFB, and 0.45 ± 0.056 *vs* 0.77 ± 0.087 in CB_1/CB_2 KO/CTRL *vs* CB_1/CB_2 KO/DNFB, for NAPE-PLD enzyme expression; and 0.51 ± 0.03 *vs* 0.45 ± 0.07 in WT/CTRL *vs* WT/DNFB, and 0.73 ± 0.013 *vs* 0.67 ± 0.05 in CB_1/CB_2 KO/CTRL *vs* CB_1/CB_2 KO/DNFB, for NAAA enzyme expression.

Expression of the mRNA for the targets of PEA in ears of DNFB-sensitized/challenged mice

Previous studies already showed that CB_2 mRNA is up-regulated in the ears of DNFB-sensitized/challenged WT mice (38). Here, we found that, in RNA samples coming from the same study in which the paraffine sections analysed earlier were obtained (38), the levels of TRPV1 mRNA measured by q-PCR, quite surprisingly, decreased, rather than increasing, following DNFB challenge. This was observed in both WT (with threshold cycles increasing from 32.78 ± 0.12 to 33.45 ± 0.34, and normalized relative expression decreasing from 1.00 ± 0.11 to 0.43 ± 0.11) and CB_1/CB_2 double KO (with threshold cycles remaining unchanged from 32.88 ± 0.21 to 32.77 ± 0.22, but with normalized relative expression decreasing from 0.89 ± 0.15 to 0.56 ± 0.10) mice. Likewise, the levels of PPARα mRNA decreased, rather than increasing, following DNFB challenge in both WT (with threshold cycles increasing from 31.78 ± 0.11 to 32.83 ± 0.11, and normalized relative expression decreasing from 0.78 ± 0.08 to 0.26 ± 0.02) and CB_1/CB_2 double KO (with threshold cycles increasing from 31.35 ± 0.04 to 31.90 ± 0.07, and normalized relative expression decreasing from 1.00 ± 0.09 to 0.40 ± 0.04) mice. Similar results (not shown) were obtained when using RNA samples prepared

from the DNFB-treated WT mice used in this study (see below).

Expression of PEA metabolic enzyme mRNA in ears of DNFB-sensitized/challenged mice

Again unexpectedly, considering that we used RNA samples coming from the same study in which the paraffine sections analysed earlier were obtained (38), the levels of NAAA mRNA, measured by q-PCR, increased, rather than decreasing, after DNFB challenge in both WT (with threshold cycles decreasing from 24.27 ± 0.17 to 22.48 ± 0.12, and normalized relative expression increasing from 0.34 ± 0.05 to 0.80 ± 0.08) and CB_1/CB_2 double KO (with threshold cycles decreasing from 23.97 ± 0.078 to 21.85 ± 0.08, and normalized relative expression increasing from 0.39 ± 0.04 to 1.00 ± 0.10) mice. The expression of NAPE-PLD mRNA, instead, decreased, rather than increasing, after DNFB challenge in both WT (with threshold cycles increasing from 27.49 ± 0.10 to 28.02 ± 0.07, and normalized relative expression decreasing from 0.87 ± 0.08 to 0.42 ± 0.03) and CB_1/CB_2 double KO (with threshold cycles increasing from 27.22 ± 0.09 to 27.43 ± 0.18, and normalized relative expression decreasing from 1.00 ± 0.10 to 0.50 ± 0.07) mice. Similar results (not shown) were obtained when using RNA samples prepared from the DNFB-treated WT mice used in this study (see below).

PEA downregulates the formation of the chemokine MCP-2 in HaCaT

Because MCP-2 down-regulation was previously shown to underlie endocannabinoid anti-inflammatory effects in CAD, and poly-(I:C) was found to reproduce *in vitro* the effects of DNFB on this chemokine *in vivo* (38), we investigated the effect of PEA on MCP-2 chemokine expression in poly-(I:C)-treated HaCaT keratinocytes. Cells treated for 24 h with poly-(I:C) produced significantly higher levels of the MCP-2 chemokine when compared to vehicle-treated HaCaT cells, in which the signal was almost undetectable (Fig. 4A). When HaCaT cells were incubated with PEA at different concentrations (0.1–1–10 μM), no effect was observed on MCP-2 chemokine expression (Fig. 4A,B), whereas, when HaCaT cells were co-stimulated with poly-(I:C) and PEA (10 μM), we observed a strong reduction of MCP-2 protein levels (Fig. 4A,B, $P < 0.001$) when compared to poly-(I:C)-treated HaCaT cells incubated with vehicle. In fact, the optical density of MCP-2-ir was 0.82 ± 0.09, 0.79 ± 0.07, 0.76 ± 0.04, 0.32 ± 0.03 *vs* 0.28 ± 0.02, 0.25 ± 0.01, 0.30 ± 0.03, 0.27 ± 0.02 respectively in VEH + POLY, POLY + PEA 0.1 μM, POLY + PEA 1.0 μM, POLY + PEA 10 μM *vs* VEH + VEH, VEH + PEA 0.1 μM, VEH + PEA 1.0 μM, VEH + PEA 10 μM.

We next investigated the effect of a CB_2 receptor antagonist (SR144528, 0.5 μM), or a TRPV1 receptor antagonist (I-RTX, 0.1 μM), or a PPAR-α receptor antagonist (MK-886, 10 μM) on MCP-2 protein levels in poly-(I:C)-sensitized HaCaT cells, in the presence or absence of PEA (10 μM). Our results show that when HaCaT cells were stimulated with the antagonists alone, no effect was observed on MCP-2 protein levels when compared to vehicle-treated HaCaT cells (Fig. 4C,D). When HaCaT cells were co-stimulated with poly-(I:C) and the antagonists alone, MCP-2 protein levels were comparable to those in the absence of the antagonists (Fig. 4C,D). In fact, the optical density of ir were 0.83 ± 0.082 *vs* 0.76 ± 0.099 in POLY *vs* POLY/SR144528-treated cells, 0.70 ± 0.075 *vs* 0.83 ± 0.089 in POLY *vs* POLY/I-RTX-treated cells, and 0.70 ± 0.075 *vs* 0.76 ± 0.089 in POLY- *vs* POLY/MK-886-treated cells. More importantly, when HaCaT cells were co-stimulated with poly-(I:C), PEA 10 μM and I-RTX, MCP-2 protein levels was comparable to those in the absence of both PEA and I-RTX (Fig. 4C,D). In fact the optical density of ir were 0.70 ± 0.075 *vs* 0.74 ± 0.065 in POLY- *vs* POLY/PEA/I-RTX-treated cells. Finally, after the co-stimulation of HaCaT cells with poly-(I:C), PEA and either SR144528 or MK-886, the extent of MCP-2 ir was comparable to that observed in the absence of SR144528 or MK-886 (Fig. 4C,D). In fact, the optical density of ir were 0.25 ± 0.013 *vs* 0.22 ± 0.013 in POLY/PEA- *vs* POLY/PEA/SR144528-treated cells, and 0.22 ± 0.015 *vs* 0.19 ± 0.021 in POLY/PEA- *vs* POLY/PEA/MK-886-treated cells.

Quantitative RT-PCR analysis of MCP-2 mRNA in HaCaT cells

MCP-2 transcriptional expression in HaCaT cells treated with poly-(I:C) at different incubation times showed a relative maximum at 6 h and a decrease to basal level at 24 h from treatment (data not shown). Table 2 shows that PEA (10 μM) inhibited the expression of MCP-2 mRNA in HaCaT cells treated with poly-(I:C) for 6 h, and that this effect was counteracted by I-RTX (0.1 μM).

ELISA assay

As shown in Fig. 4E, PEA (10 μM) inhibited the release of MCP-2 into the medium of HaCaT cells treated with poly-(I:C) for 6 h. The effect was counteracted by I-RTX (0.1 μM).

AEA, PEA and OEA content in poly-(I:C)-sensitized HaCaT cells

In order to investigate the possibility of an 'entourage' effect at TRPV1 receptors as a molecular mechanism for PEA action, we determined the levels of AEA, 2-AG, PEA and the other endovanilloid and endogenous PPAR-α ligand, OEA in poly-(I:C)-treated HaCaT cells. Our results, shown in Fig. 5, indicate that AEA levels are elevated in poly-(I:C)-treated HaCaT cells (0.39 ± 0.13 pmol/mg of lipid extract) when compared to vehicle-treated HaCaT cells (0.08 ± 0.02 pmol/mg of lipid extract). PEA and OEA levels were even more strongly elevated in poly-(I:C)-treated HaCaT cells (10.18 ± 1.06 pmol/mg and 29.77 ± 1.61 pmol/mg of lipid extract) when compared to vehicle-treated HaCaT cells

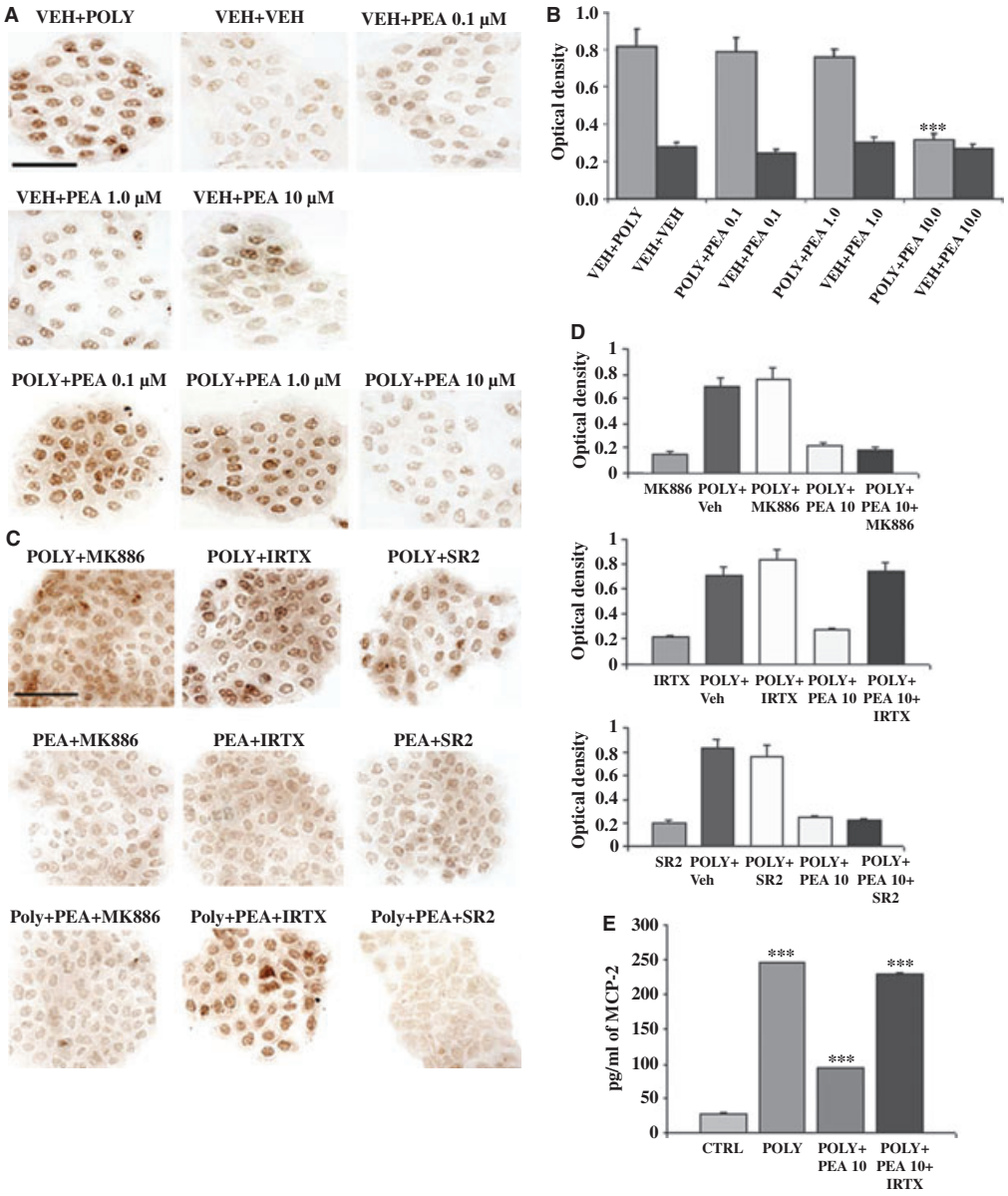

Figure 4 MCP-2 chemokine expression in polyinosinic polycytidylic acid [poly-(I:C)]-stimulated human keratinocytes (HaCaT) cells. (A) 3-3′diaminobenzidine (DAB) labelling for MCP2-immunoreactivity in the presence or in the absence of palmitoylethanolamide (PEA) at different concentrations (0.1–1–10 μM) in cells stimulated for 24 h with poly-(I:C) (100 μg/ml, POLY). Scale bar = 100 μm. (B) Histograms of the densitometric analyses of experiments such as those depicted in (A). Data are means ± SD of $N = 3$ separate determinations on $n = 100$ cells. ***$P < 0.001$ for VEH + POLY or POLY + PEA 0.1 μM or POLY + PEA 1.0 μM *vs* POLY + PEA 10.0 μM. (C) DAB labelling for MCP-2-ir in the presence of the antagonists MK-886 (10 μM), iodio-resiniferatoxin (IRTX, 0.1 μM) and SR144528 (SR2, 0.5 μM), in the presence or in the absence of PEA (10 μM), in cells stimulated for 24 h with poly-(I:C) (100 μg/ml, POLY). Scale bar = 100 μm. (D) Histograms of the densitometric analyses of experiments such as those depicted in (C). Upper panel: $P < 0.001$ for MK866 *vs* POLY + VEH or POLY + MK866; $P < 0.01$ for POLY + VEH *vs* POLY + PEA 10.0 μM or POLY + PEA 10.0 μM + MK866; $P < 0.01$ for POLY + MH866 *vs* POLY + PEA 10.0 μM or POLY + PEA 10.0 μM + MK866. Middle panel: $P < 0.001$ for IRTX *vs* POLY + VEH or POLY + IRTX; $P < 0.01$ for POLY + VEH *vs* POLY + PEA 10.0 μM or POLY + PEA10.0 μM + IRTX; $P < 0.01$ for POLY + IRTX *vs* POLY + PEA 10.0 μM or POLY + PEA 10.0 μM + IRTX. Lower panel: $P < 0.001$ for SR2 *vs* POLY + VEH or POLY + SR2; $P < 0.01$ for POLY + VEH *vs* POLY + PEA 10.0 μM or POLY + PEA 10.0 μM + SR2; $P < 0.01$ for POLY + SR2 *vs* POLY + PEA 10.0 μM or POLY + PEA 10.0 μM + SR2. Data in (B,D) are means ± SD of $N = 3$ separate determinations on $n = 100$ cells. (E) ELISA assay for MCP-2 in the supernatants of poly-(I:C)-(100 μg/ml, POLY)-stimulated HaCaT cells (6-h incubation). Data are means ± SE of $N = 3$ separate determinations. ***$P < 0.001$ control *vs* POLY and POLY *vs* POLY + PEA 10 μM and POLY + PEA 10 μM *vs* POLY + PEA 10 μM + IRTX.

Table 2 MCP-2 transcriptional expression in human keratinocytes (HaCaT) cells treated for 6 h with polyinosinic polycytidylic acid (100 μg/ml, POLY), PEA (10 μM) and I-RTX (0.1 μM). HaCaT cells were cultured in presence of POLY, PEA and I-RTX, as described in Materials and methods. Total RNA was extracted and assayed by quantitative RT-PCR for MCP-2 and β-actin (reference gene) targets, as described in Materials and methods

Condition	Gene	Mean threshold cycles	SD	Relative quantity	SD	Normalized relative expression	SD
CTRL	β-Actin	19.39	0.19131	1.00000	0.13260	NA	NA
	MCP-2	24.57	0.22326	1.00000	0.15475	1.00000	0.20379
POLY	β-Actin	25.53	0.19867	0.01420	0.00195	NA	NA
	MCP-2	24.81	0.26314	0.85006	0.15505	59.88177*	13.68563
PEA	β-Actin	19.62	0.05211	0.85394	0.03084	NA	NA
	MCP-2	25.85	0.80724	0.41273	0.23094	0.48332	0.27100
POLY+PEA	β-Actin	19.76	0.14561	0.77120	0.07784	NA	NA
	MCP-2	25.83	0.57063	0.41924	0.16582	0.54361	0.22190
IRTX	β-Actin	19.31	0.03000	1.05538	0.02195	NA	NA
	MCP-2	25.19	0.88306	0.65196	0.39906	0.61775	0.37834
POLY+PEA+IRTX	β-Actin	24.09	0.13715	0.03838	0.00365	NA	NA
	MCP-2	25.77	0.47254	0.43593	0.14278	11.35825*,**	3.87381

Relative quantity, relative quantity *vs* the sample in which the gene was most highly expressed; normalized relative expression, normalized expression with respect to β-actin; SD, standard deviation; I-RTX, iodio-resiniferatoxin; PEA, palmitoylethanolamide.
*$P < 0.005$ *vs* control (CTRL); **$P < 0.05$ *vs* POLY.

(1.92 ± 0.12 and 5.56 ± 0.57 pmol/mg of lipid extract). By contrast, the levels of the endocannabinoid 2-AG, which has no activity at TRPV1 receptors, were significantly reduced in poly-(I:C)-treated HaCaT cells.

Effect of PEA in mice with DNFB-induced CAD

The i.p. administration of PEA at the doses of 5 and 10 mg/kg on day 5, 6 and 7 significantly reduced, although not in a dose-dependent way, the ear thickness measured 24, 48 and 72 h after the first challenge when compared to CTRL mice (Fig. 6A). On the contrary, only PEA at the highest dose (10 mg/kg) administered on day 12, 13 and 14 reduced ear thickness measured 24, 48 and 72 h after the second challenge, whereas in this case the 5 mg/kg dose did not show any effect (Fig. 6A). The co-administration of *per se* inactive doses of cpz (0.5–2 mg/kg) with PEA (5–10 mg/kg) was able to reverse PEA effect on ear thickness exclusively only after the first challenge (Fig. 6B,C). In agreement with previous data (38), the first challenge with DNFB also caused a strong increase in MCP-2 mRNA expression in inflamed ears (Table 1). This effect was significantly counteracted by co-treatment with 5 mg/kg PEA on day 5, 6 and 7 (Table 1).

Discussion

In this study, we demonstrated for the first time, a protective role of PEA against inflammation in an experimental model of CAD *in vivo*, and in keratinocytes *in vitro*, and investigated the molecular mechanism for the actions of PEA *in vitro*.

First, we showed that strongly elevated levels of PEA are found particularly in the ear skin of the same DNFB-treated CB_1/CB_2 double KO mice previously reported to display a dramatically stronger inflammatory response to DNFB (38). Therefore, the extent to which PEA levels are increased after challenge with DNFB appears to correspond to the extent of the inflammatory response. The increased endogenous levels of PEA were accompanied, specifically in ear skin keratinocytes, by the up-regulation of NAPE-PLD, the enzyme responsible of the biosynthesis of this mediator, and by the slight down-regulation of NAAA, one of the enzymes catalysing PEA inactivation. These changes in the protein levels of these enzymes suggest that the metabolic machinery regulating PEA concentration is modified during DNFB-induced CAD in order to increase the concentration of this compound selectively in keratinocytes. Indeed, when we quantified, in whole ear tissue, the mRNA levels of NAPE-PLD and NAAA by q-PCR, we found that, opposite to what observed in keratinocytes using immunostaining, the two enzymes were respectively down- and up-regulated following DNFB-induced inflammation. Assuming, bona fide, the specificity of the antibodies used here for the immunohistochemical experiments, this finding can be interpreted by hypothesizing that, in other cell types participating in DNFB-induced CAD, such as mast cells, macrophages and CD8+ T cells, that may have not been detectable in the slices used for immunostaining experiments (which normally contain much less tissue than that used for q-PCR determination), the enzymatic machinery controlling PEA levels is regulated in a way opposite to that observed in keratinocytes. This, in turn, might lead to a localized decrease of PEA levels in mast cells, macrophages and/or CD8+ T cells that would not be sufficient to cause a global decrease of PEA in the inflamed ears, but, given the anti-inflammatory effects of PEA (32, 46), might still contribute to the activation of these immune cells and/or their migration towards the site of inflammation. This hypothesis should be evaluated, for example, by isolating CD8+ T cells infiltrating the skin following DNFB

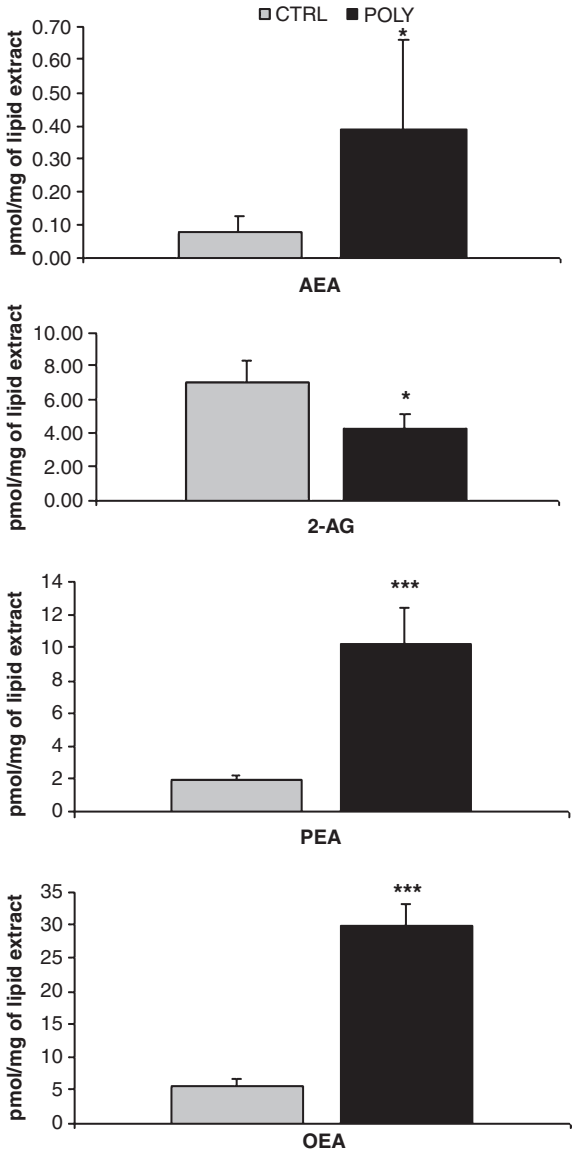

Figure 5 Endocannabinoid [anandamide (AEA), 2-arachidonoylglycerol (2-AG)], palmitoylethanolamide (PEA) and oleoylethanolamide (OEA) levels in polyinosinic polycytidylic acid [poly-(I:C)]-(100 μg/ml, POLY)-stimulated human keratinocytes cells (24-h incubation). Data are means ± SE of $N = 3$ separate determinations. AEA and 2-AG: $^{*}P < 0.05$ for control (CTRL) *vs* POLY-(I:C); PEA and OEA: $^{***}P < 0.001$ for CTRL *vs* POLY-(I:C).

challenge (as well as the draining lymph node responsible for their release), and measuring their PEA content and the effect of PEA on their proliferation and priming. Such experiments, whilst being outside the scope of the present study, which was aimed at investigating the regulation and role of PEA in keratinocytes, should be undertaken in the future.

The up-regulation of PEA levels observed here after DNFB treatment is reminiscent of that previously reported by us for the levels of the two endocannabinoids, AEA and 2-AG, in the same animal model (38). In fact, these two compounds are also elevated in the ear skin of DNFB-treated WT and, particularly, CB_1/CB_2 double KO mice, and were suggested to exert a protective role against CAD by acting on keratinocytes via CB_1 and CB_2 receptors (38). Therefore, our next experiments were aimed at investigating if also PEA plays a similar protective function in keratinocytes. First, we observed that TRPV1 and PPAR-α receptors, which are known to be over-expressed in human and murine epidermal keratinocytes under certain inflammatory conditions (47, 48), are over-expressed also in the keratinocytes of the ears of DNFB-sensitized and challenged mice. We also confirmed the previous finding that a similar up-regulation occurs also for CB_2 receptors (38), which, together with TRPV1 and PPAR-α, is another proposed direct or indirect target for PEA. The up-regulation of TRPV1 and PPAR-α is likely specific for keratinocytes, because q-PCR analysis of the mRNAs encoding the two proteins revealed that, instead, they are down-regulated in the ear tissue of DNFB-treated mice. These data suggest that PEA, produced by keratinocytes during DNFB-induced CAD, might act at either CB_2, TRPV1 or PPAR-α receptors mostly on these cells, in an autocrine way. To investigate what type of role PEA might play in keratinocytes, and through what receptor, we used cultures of HaCaT keratinocytes, which express cannabinoid, PPAR-α and TRPV1 receptors, as well as the enzymatic apparatus necessary for PEA biosynthesis and degradation (49–51; P. Orlando and V. Di Marzo, unpublished data). Importantly, when stimulated with poly-(I:C) (an agonist of the toll-like receptor 3), HaCaT cells produce MCP-2 (38). This chemokine (1) is involved in the recruitment of macrophages and mast cells into inflammatory sites, and in the activation of T-lymphocytes (52, 53) and (2) even more relevant to the present study, is the same pro-inflammatory mediator the down-regulation of which underlies the anti-inflammatory effects of CB_1/CB_2 agonists in ear keratinocytes of mice with DNFB-induced CAD, as well as in poly-(I:C)-treated HaCaT cells *in vitro* (38). Therefore, we assessed whether also PEA inhibits MCP-2 expression in HaCaT keratinocytes. Indeed, PEA did reduce (1) MCP-2 protein levels in HaCaT cells stimulated for 24 h with poly-(I:C); and (2) MCP-2 mRNA levels and MCP-2 protein release after a 6-h stimulation with poly-(I:C). In order to investigate whether this protective action was receptor mediated, we studied the effect of antagonists of the proposed PEA targets. We found that only a selective antagonist of TRPV1 receptors, I-RTX, was able to reverse the inhibitory effect of PEA on MCP-2 expression, whereas this effect was not influenced by either CB_2 or PPAR-α receptors antagonists. These data indicate that PEA, like the endocannabinoids (38), but through a different molecular mechanism, is able to counteract MCP-2 production and release by cultured HaCaT cells.

Given the lack of activity *per se* of PEA at TRPV1 receptors, our *in vitro* pharmacological experiments suggest that this mediator might exert its autocrine protective action in keratinocytes by an 'entourage' effect on endogenous ligands of TRPV1 receptors, such as AEA and OEA (54), as previously hypothesized also for other effects of PEA both *in vitro*

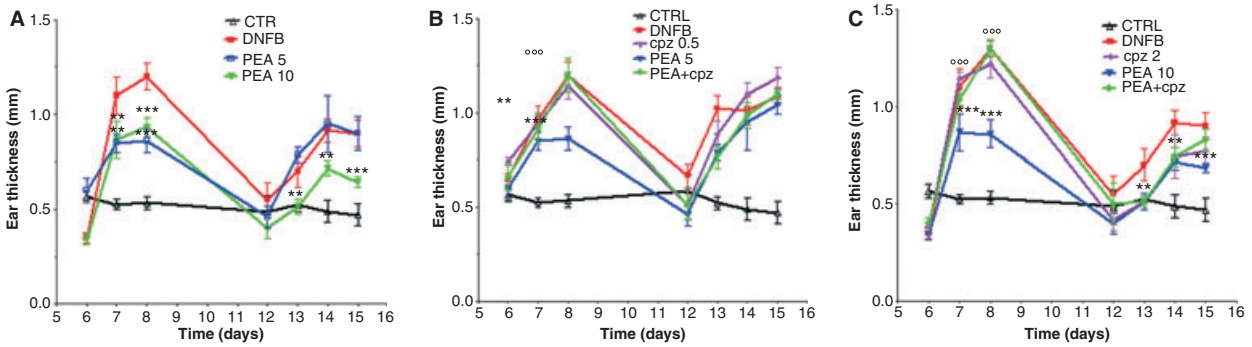

Figure 6 Effect of intra-peritoneal administration of (A) Palmitoylethanolamide (PEA) (5 mg/kg and 10 mg/kg), (B) PEA (5 mg/kg) with or without capsazepine (cpz, 0.5 mg/kg), (C) PEA (10 mg/kg) with or without cpz (2 mg/kg) in 2,4-dinitrofluorobenzene (DNFB)-sensitized and challenged mice (see Materials and methods). Results are shown as mean ± SE of $N = 11$ mice. Two-way anova was used followed by *post hoc* testing. $^{**}P < 0.01$, $^{***}P < 0.001$ *vs* DNFB-sensitized mice; $^{\circ\circ}P < 0.01$, $^{\circ\circ\circ}P < 0.001$ *vs* PEA-treated sensitized mice.

and *in vivo* (27, 28). Therefore, we determined whether HaCaT cells do produce AEA and OEA. We show that the levels of AEA, OEA and PEA are significantly elevated after 24-h stimulation of HaCaT cells with poly-(I:C), whereas a decrease was instead observed for the levels of 2-AG, which does not activate TRPV1 receptors. These data support our hypothesis that PEA might act on poly-(I:C)-treated keratinocytes via an 'entourage' effect on AEA- and OEA-mediated TRPV1 receptor activation/desensitization. They are in agreement with (1) the previously reported capability of PEA to potentiate endovanilloid activation of TRPV1 receptors (25, 26, 55, 56); (2) the proposed pro-inflammatory role of TRPV1 in keratinocytes (50, 57) and (3) the anti-inflammatory actions of TRPV1 agonists/desensitizers and antagonists (58).

Finally, we wanted to gain evidence that the anti-inflammatory effect of PEA occurs also *in vivo* in the same model of CAD in which the compound is up-regulated. We found that PEA reduced the DNFB-induced ear skin oedema, which was shown previously to be partly mediated by MCP-2 (38). Accordingly, we also found that PEA reduces significantly DNFB-induced elevation of MCP-2 mRNA levels in ear skin. Importantly, the anti-inflammatory effect of PEA on the first, but not on the second, challenge was counteracted by *per se* inactive doses of the TRPV1 antagonist, capsazepine. This indicates that the mechanism of PEA anti-inflammatory effect observed *in vitro* in keratinocytes might apply also to DNFB-sensitized mice, at least for what the first challenge is concerned. However, although keratinocytes play an important role in all phases of CAD, especially in the early initiation phase, it is also well known that the inflammatory response that follows subsequent challenges involves different cell types, such as T-lymphocytes and mast cells. Therefore, further studies will be needed to investigate the molecular target(s) and cell types involved in the protective actions of PEA in this animal model of CAD, particularly as we provided here no evidence that the anti-oedema and MCP-2-down-regulatory effects of this compound *in vivo* are because of interaction with keratinocytes and not, for example, CD8+ T cells or mast cells.

In conclusion, we have presented data suggesting that (1) ear skin keratinocytes are possibly the major cellular source of the strongly elevated PEA tissue levels detected in the ears of DNFB-sensitized/challenged mice, an animal model of CAD; (2) PEA levels are also elevated, together with the levels of the related endocannabinoid/endovanilloids, AEA and OEA, in cultured HaCaT following the treatment with poly-(I:C) and (3) PEA down-regulates the expression and levels of the inflammatory cytokine MCP-2 in poly-(I:C)-treated HaCaT *in vitro* in a way antagonized by a selective TRPV1 antagonist, and exerts an anti-inflammatory action in DNFB-sensitized/challenged mice, again partly via TRPV1 receptors. Future studies will have to investigate what additional molecular and cellular targets of PEA are involved in its anti-inflammatory actions in this and other animal models of CAD. Our findings might open the way to the future testing of PEA in human CAD.

Conflict of interest

The authors state no conflict of interest.

Acknowledgments

This work was partly supported by Epitech Group S.r.l. The authors are grateful to Dr Katarzyna Starowicz and Marco Allarà for technical assistance.

References

1. Grabbe S, Schwarz T. Immunoregulatory mechanisms involved in elicitation of allergic contact hypersensitivity. *Immunol Today* 1998;**19**:37–44.
2. Krasteva M, Kehren J, Ducluzeau MT, Sayag M, Cacciapuoti M, Akiba H et al. Contact dermatitis I pathophysiology of contact sensitivity. *Eur J Dermatol* 1999;**9**:65–77.
3. Di Marzo V, De Petrocellis L, Sepe N, Buono A. Biosynthesis of anandamide and related acylethanolamides in mouse J774

macrophages and N18 neuroblastoma cells. *Biochem J* 1996;**316**:977–984.
4. Bisogno T, Maurelli S, Melck D, De Petrocellis L, Di Marzo V. Biosynthesis, uptake, and degradation of anandamide and palmitoylethanolamide in leukocytes. *J Biol Chem* 1997;**272**:3315–3323.
5. Berdyshev EV, Boichot E, Germain N, Allain N, Anger JP, Lagente V. Influence of fatty acid ethanolamides and delta9-tetrahydrocannabinol on cytokine and arachidonate release by mononuclear cells. *Eur J Pharmacol* 1997;**330**:231–240.
6. Calignano A, La Rana G, Giuffrida A, Piomelli D. Control of pain initiation by endogenous cannabinoids. *Nature* 1998;**394**:277–281.
7. Jaggar SI, Hasnie FS, Sellaturay S, Rice AS. The anti-hyperalgesic actions of the cannabinoid anandamide and the putative CB2 receptor agonist palmitoylethanolamide in visceral and somatic inflammatory pain. *Pain* 1998;**76**:189–199.
8. Calignano A, La Rana G, Piomelli D. Antinociceptive activity of the endogenous fatty acid amide, palmitylethanolamide. *Eur J Pharmacol* 2001;**419**:191–198.
9. Costa B, Conti S, Giagnoni G, Colleoni M. Therapeutic effect of the endogenous fatty acid amide, palmitoylethanolamide, in rat acute inflammation: inhibition of nitric oxide and cyclo-oxygenase systems. *Br J Pharmacol* 2002;**137**:413–420.
10. Darmani NA, Izzo AA, Degenhardt B, Valenti M, Scaglione G, Capasso R et al. Involvement of the cannabimimetic compound, *N*-palmitoyl-ethanolamine, in inflammatory and neuropathic conditions: review of the available pre-clinical data, and first human studies. *Neuropharmacology* 2005;**48**:1154–1163.
11. Okamoto Y, Morishita J, Tsuboi K, Tonai T, Ueda N. Molecular characterization of a phospholipase D generating anandamide and its congeners. *J Biol Chem* 2004;**279**:5298–5305.
12. Cravatt BF, Giang DK, Mayfield SP, Boger DL, Lerner RA, Gilula NB. Molecular characterization of an enzyme that degrades neuromodulatory fatty-acid amides. *Nature* 1996;**384**:83–87.
13. Bracey MH, Hanson MA, Masuda KR, Stevens RC, Cravatt BF. Structural adaptations in a membrane enzyme that terminates endocannabinoid signaling. *Science* 2002;**298**:1793–1796.
14. Ueda N, Yamanaka K, Terasawa Y, Yamamoto S. An acid amidase hydrolyzing anandamide as an endogenous ligand for cannabinoid receptors. *FEBS Lett* 1999;**454**:267–270.
15. Ueda N, Yamanaka K, Yamamoto S. Purification and characterization of an acid amidase selective for *N*-palmitoylethanolamine, a putative endogenous anti-inflammatory substance. *J Biol Chem* 2001;**276**:35552–35557.
16. Aloe L, Leon A, Levi-Montalcini R. A proposed autacoid mechanism controlling mastocyte behaviour. *Agents Actions* 1993;**39**:C145–C147.
17. Facci L, Dal Toso R, Romanello S, Buriani A, Skaper SD, Leon A. Mast cells express a peripheral cannabinoid receptor with differential sensitivity to anandamide and palmitoylethanolamide. *Proc Natl Acad Sci USA* 1995;**92**:3376–3380.
18. Mazzari S, Canella R, Petrelli L, Marcolongo G, Leon A. *N*-(2-hydroxyethyl)hexadecanamide is orally active in reducing edema formation and inflammatory hyperalgesia by down-modulating mast cell activation. *Eur J Pharmacol* 1996;**300**:227–236.
19. Berdyshev EV, Schmid PC, Dong Z, Schmid HH. Stress-induced generation of *N*-acylethanolamines in mouse epidermal JB6 P+ cells. *Biochem J* 2000;**346**:369–374.
20. Conti S, Costa B, Colleoni M, Parolaro D, Giagnoni G. Antiinflammatory action of endocannabinoid palmitoylethanolamide and the synthetic cannabinoid nabilone in a model of acute inflammation in the rat. *Br J Pharmacol* 2002;**135**:181–187.
21. Farquhar-Smith WP, Rice AS. A novel neuroimmune mechanism in cannabinoid-mediated attenuation of nerve growth factor-induced hyperalgesia. *Anesthesiology* 2003;**99**:1391–1401.
22. Ben-Shabat S, Fride E, Sheskin T, Tamiri T, Rhee MH, Vogel Z et al. An entourage effect: inactive endogenous fatty acid glycerol esters enhance 2-arachidonoyl-glycerol cannabinoid activity. *Eur J Pharmacol* 1998;**353**:23–31.
23. Lambert DM, Di Marzo V. The palmitoylethanolamide and oleamide enigmas : are these two fatty acid amides cannabimimetic? *Curr Med Chem* 1999;**6**:757–773.
24. Di Marzo V, Melck D, Orlando P, Bisogno T, Zagoory O, Bifulco M et al. Palmitoylethanolamide inhibits the expression of fatty acid amide hydrolase and enhances the antiproliferative effect of anandamide in human breast cancer cells. *Biochem J* 2001;**358**:249–255.
25. De Petrocellis L, Davis JB, Di Marzo V. Palmitoylethanolamide enhances anandamide stimulation of human vanilloid VR1 receptors. *FEBS Lett* 2001;**506**:253–256.
26. Smart D, Jonsson KO, Vandevoorde S, Lambert DM, Fowler CJ. 'Entourage' effects of *N*-acyl ethanolamines at human vanilloid receptors. Comparison of effects upon anandamide-induced vanilloid receptor activation and upon anandamide metabolism. *Br J Pharmacol* 2002;**136**:452–458.
27. Ho WS, Barrett DA, Randall MD. 'Entourage' effects of *N*-palmitoylethanolamide and *N*-oleoylethanolamide on vasorelaxation to anandamide occur through TRPV1 receptors. *Br J Pharmacol* 2008;**155**:837–846.
28. Costa B, Comelli F, Bettoni I, Colleoni M, Giagnoni G. The endogenous fatty acid amide, palmitoylethanolamide, has anti-allodynic and anti-hyperalgesic effects in a murine model of neuropathic pain: involvement of CB(1), TRPV1 and PPAR gamma receptors and neurotrophic factors. *Pain* 2008;**139**:541–550.
29. Szallasi A, Blumberg PM, Annicelli LL, Krause JE, Cortright DN. The cloned rat vanilloid receptor VR1 mediates both R-type binding and C-type calcium response in dorsal root ganglion neurons. *Mol Pharmacol* 1999;**56**:581–587.
30. Zygmunt PM, Petersson J, Andersson DA, Chuang H, Sørgård M, Di Marzo V et al. Vanilloid receptors on sensory nerves mediate the vasodilator action of anandamide. *Nature* 1999;**400**:452–457.
31. Smart D, Gunthorpe MJ, Jerman JC, Nasir S, Gray J, Muir AI et al. The endogenous lipid anandamide is a full agonist at the human vanilloid receptor (hVR1). *Br J Pharmacol* 2000;**129**:227–230.
32. Lo Verme J, Fu J, Astarita G, La Rana G, Russo R, Calignano A et al. The nuclear receptor peroxisome proliferator-activated receptor-alpha mediates the anti-inflammatory actions of palmitoylethanolamide. *Mol Pharmacol* 2005;**67**:15–19.
33. Lo Verme J, Russo R, La Rana G, Fu J, Farthing J, Mattace-Raso G et al. Rapid broad-spectrum analgesia through activation of peroxisome proliferator-activated receptor-alpha. *J Pharmacol Exp Ther* 2006;**319**:1051–1061.
34. Lambert DM. Allergic contact dermatitis and the endocannabinoid system: from mechanisms to skin care. *Chem MedChem* 2007;**2**:1701–1702.
35. Oka S, Wakui J, Ikeda S, Yanagimoto S, Kishimoto S, Gokoh M et al. Involvement of the cannabinoid CB2 receptor and its endogenous ligand 2-arachidonoylglycerol in oxazolone-induced contact dermatitis in mice. *J Immunol* 2006;**177**:8796–8805.
36. Iwamura H, Suzuki H, Ueda Y, Kaya T, Inaba T. In vitro and in vivo pharmacological characterization of JTE-907, a novel selective ligand for cannabinoid CB2 receptor. *J Pharmacol Exp Ther* 2001;**296**:420–425.
37. Ueda Y, Miyagawa N, Matsui T, Kaya T, Iwamura H. Involvement of cannabinoid CB(2) receptor-mediated response and efficacy of cannabinoid CB(2) receptor inverse agonist, JTE-907, in cutaneous inflammation in mice. *Eur J Pharmacol* 2005;**520**:164–171.

38. Karsak M, Gaffal E, Date R, Wang-Eckhardt L, Rehnelt J, Petrosino S et al. Attenuation of allergic contact dermatitis through the endocannabinoid system. *Science* 2007;**316**:1494–1497.
39. Bánvölgyi A, Pálinkás L, Berki T, Clark N, Grant AD, Helyes Z et al. Evidence for a novel protective role of the vanilloid TRPV1 receptor in a cutaneous contact allergic dermatitis model. *J Neuroimmunol* 2005;**169**:86–96.
40. Tsuboi K, Zhao LY, Okamoto Y, Araki N, Ueno M, Sakamoto H et al. Predominant expression of lysosomal *N*-acylethanolamine-hydrolyzing acid amidase in macrophages revealed by immunochemical studies. *Biochim Biophys Acta* 2007;**1771**:623–632.
41. Bisogno T, Sepe N, Melck D, Maurelli S, De Petrocellis L, Di Marzo V. Biosynthesis, release and degradation of the novel endogenous cannabimimetic metabolite 2-arachidonoylglycerol in mouse neuroblastoma cells. *Biochem J* 1997;**322**:671–677.
42. Marsicano G, Wotjak CT, Azad SC, Bisogno T, Rammes G, Cascio MG et al. The endogenous cannabinoid system controls extinction of aversive memories. *Nature* 2002;**418**:530–534.
43. Di Marzo V, Goparaju SK, Wang L, Liu J, Batkai S, Jarai Z et al. Leptin-regulated endocannabinoids are involved in maintaining food intake. *Nature* 2001;**410**:822–825.
44. Stabile M, Angelino T, Caiazzo F, Olivieri P, De Marchi N, De Petrocellis L et al. Fertility in a i(Xq) Klinefelter patient: importance of XIST expression level determined by qRT-PCR in ruling out Klinefelter cryptic mosaicism as cause of oligozoospermia. *Mol Hum Reprod* 2008;**14**:635–640.
45. Pfaffl MW, Horgan GW, Dempfle L. Relative expression software tool (REST) for group-wise comparison and statistical analysis of relative expression results in real-time PCR. *Nucleic Acids Res* 2002;**30**:e36.
46. Re G, Barbero R, Miolo A, Di Marzo V. Palmitoylethanolamide, endocannabinoids and related cannabimimetic compounds in protection against tissue inflammation and pain: potential use in companion animals. *Vet J* 2007;**173**:21–30.
47. Ständer S, Moormann C, Schumacher M, Buddenkotte J, Artuc M, Shpacovitch V et al. Expression of vanilloid receptor subtype 1 in cutaneous sensory nerve fibers, mast cells, and epithelial cells of appendage structures. *Exp Dermatol* 2004;**13**:129–139.
48. Michalik L, Desvergne B, Tan NS, Basu-Modak S, Escher P, Rieusset J et al. Impaired skin wound healing in peroxisome proliferator-activated receptor (PPAR)alpha and PPARbeta mutant mice. *Biol Cell* 2001;**154**:799–814.
49. Maccarrone M, Di Rienzo M, Battista N, Gasperi V, Guerrieri P, Rossi A et al. The endocannabinoid system in human keratinocytes. Evidence that anandamide inhibits epidermal differentiation through CB1 receptor-dependent inhibition of protein kinase C, activation protein-1, and transglutaminase. *J Biol Chem* 2003;**278**:33896–33903.
50. Li WH, Lee YM, Kim JY, Kang S, Kim S, Kim KH et al. Transient receptor potential vanilloid-1 mediates heat-shock-induced matrix metalloproteinase-1 expression in human epidermal keratinocytes. *J Invest Dermatol* 2007;**127**:2328–2335.
51. Lim SW, Hong SP, Jeong SW, Kim B, Bak H, Ryoo HC et al. Simultaneous effect of ursolic acid and oleanolic acid on epidermal permeability barrier function and epidermal keratinocyte differentiation via peroxisome proliferator-activated receptor-alpha. *J Dermatol* 2007;**34**:625–634.
52. Taub DD, Proost P, Murphy WJ, Anver M, Longo DL, van Damme J et al. Monocyte chemotactic protein-1 (MCP-1), -2, and -3 are chemotactic for human T lymphocytes. *J Clin Invest* 1995;**95**:370–1376.
53. de Paulis A, Annunziato F, Di Gioia L, Romagnani S, Carfora M, Beltrame C et al. Expression of the chemokine receptor CCR3 on human mast cells. *Int Arch Allergy Immunol* 2001;**124**:146–150.
54. Movahed P, Jönsson BA, Birnir B, Wingstrand JA, Jørgensen TD, Ermund A et al. Endogenous unsaturated C18 *N*-acylethanolamines are vanilloid receptor (TRPV1) agonists. *J Biol Chem* 2005;**280**:38496–38504.
55. Vandevoorde S, Lambert DM, Smart D, Jonsson KO, Fowler CJ. *N*-Morpholino- and *N*-diethyl-analogues of palmitoylethanolamide increase the sensitivity of transfected human vanilloid receptors to activation by anandamide without affecting fatty acid amidohydrolase activity. *Bioorg Med Chem* 2003;**11**:817–825.
56. García Mdel C, Adler-Graschinsky E, Celuch SM. Enhancement of the hypotensive effects of intrathecally injected endocannabinoids by the entourage compound palmitoylethanolamide. *Eur J Pharmacol* 2009;**610**:75–80.
57. Facer P, Casula MA, Smith GD, Benham CD, Chessell IP, Bountra C et al. Differential expression of the capsaicin receptor TRPV1 and related novel receptors TRPV3, TRPV4 and TRPM8 in normal human tissues and changes in traumatic and diabetic neuropathy. *BMC Neurol* 2007; **7**:11.
58. Gunthorpe MJ, Szallasi A. Peripheral TRPV1 receptors as targets for drug development: new molecules and mechanisms. *Curr Pharm Des* 2008;**14**:32–41.